Computer simulation of a CF_4 plasma etching silicon

David Edelson and Daniel L. Flamm
AT&T Bell Laboratories, Murray Hill, New Jersey 07974

(Received 28 December 1983; accepted for publication 30 March 1984)

A CF_4 plasma etching silicon has been simulated to identify dominant chemical processes and to quantify the effects of various reaction and transport parameters. The model was a one-dimensional plug-flow reactor in which a packet of gas is followed through the plasma and into the afterglow region, allowing the simulation to be performed as an initial value problem in ordinary differential equations. Two temperature zones were used with all known significant reactions incorporated into the chemical mechanism with the best available rate constants. Adjustable parameters were included only for certain sticking coefficients, surface recombination rates, and surface polymerization rates. Appropriate adjustment of these parameters gives satisfactory agreement between the simulations and experimental measurements of downstream gas-phase composition. The model unambiguously shows that fluorine atoms are the main reactive species in the plasma, that gas phase chemistry is clearly dominated by neutral reactions, and that formation of surface polymer has a strong effect on the composition of the gas phase. A full sensitivity analysis of the mechanism reveals that transport processes, surface chemistry, and the formation of fluorocarbon polymer on the walls are among the dominant components of the mechanism, but adequate data for these are unavailable. It is concluded that improvements in the model will require the inclusion of three-dimensional spatial dependencies and better information on surface processes.

I. INTRODUCTION

At the present time, control of the many factors affecting plasma processing (e.g., gas composition, pressure, temperature, discharge frequency, power, reactor geometry, and flow pattern) is largely empirical.[1] The chemistry of the plasma itself is incompletely understood and our knowledge of surface interactions is poor. However, we have long held that the total description of a process need not be a prerequisite for the construction and study of a detailed model, and that even in rudimentary form, a model can show the extent to which current knowledge is consistent with experiment, and can often pinpoint specific gaps which must be filled in order to complete the picture.[2]

With this philosophy in mind, we have assembled a detailed chemical and flow model of a relatively simple plasma processing system: CF_4 etching silicon. There is a considerable literature on the chemistry of ions and molecular fragments in this gas, or for analogous compounds from which behavior can be extrapolated. By using a simplified flow field and parameterizing unknown quantities, a preliminary model can be built which shows most features of the real system. Sensitivity analysis can then provide information on the relative importance of various components of the mechanism and can indicate the refinements needed to improve the model for use in prediction and process control.

II. THE MODEL

A. Flow model

As a first approximation to the complicated geometry and flow pattern of a production plasma reactor, we have assumed plug flow in a cylindrical tube. This configuration has been used in laboratory studies of plasma chemistry[3] and to generate reactive species for "downstream etching." A cylindrical packet of gas (a "plug") of length Δx flows axially along the tube, and is considered to be well mixed across its diameter. The gas enters the plasma region at time 0 and exits at time $t_f = l/v$, where l is the length of the plasma region and v the flow velocity. Thus time and space coordinates can be interchanged, and the simulation reduced to an initial-value problem in ordinary differential equations with time the only independent variable. The space beyond the plasma region (the "afterglow") may also be included in the computation so that the decay of reactive species toward equilibrium is observed downstream.

The numerical solution is stopped at a time corresponding to the exit from the plasma region; parameter values are reset to those appropriate to the afterglow and the computation is resumed. This effectively imposes an abrupt change in conditions, especially temperature, at the edge of the plasma zone, rather than a gradual transition. However, charged species concentrations and electron temperature do in fact decay rapidly in this zone and this approximation should be good for the present purposes.

B. Plasma model

The plasma is assumed to be a source of ionization that produces electrons and ions in the region according to the equation

$$CF_4 \rightarrow CF_3^+ + F + e^-. \quad (1)$$

Other ions are neglected because CF_3^+ is by far the predominant ion in CF_4 (Refs. 4 and 5) and CF_4/O_2 (Ref. 6) and homologous fluorocarbon discharges[7] and the mole fraction of silicon-containing compounds in the gas phase is low. Loss of the charged species proceeds by homogeneous reaction (e.g., R11, R16) and ambipolar diffusion to the walls, and subsequent surface recombination according to reactions R34–38 in Table I (see Sec. II C); the source intensity is adjusted to maintain the plasma density at a preset value.

DOCKET ALARM Find authenticated court documents without watermarks at docketalarm.com.

TABLE I. CF_4 Plasma etching mechanism.

No.	Reaction	Rate expression	k_{Plasma}	$k_{Afterglow}$	Ref.	Relative ser					
						Flow ~ 7 $cm^3\ min^{-1}$				Flow ~ 25	
						C_2F_6	F	F_2	SiF_4	C_2F_6	F
	Gas phase reactions										
1	$e^- + CF_4 \rightarrow CF_3 + F + e^-$	Parameter	1.00×10^{-10}	0.0	a	10	10	10		10	10
						10	*5*	*9*	*7*	*10*	*8*
2	$CF_3 + F + M \rightarrow CF_4 + M$	Parameter	3.50×10^{-32}	3.50×10^{-32}		1	1	1			
3	$2CF_3 \rightarrow C_2F_6(^*)$	$2.002\times10^{-14}T - 3.462\times10^{-13}$	5.92×10^{-12}	5.62×10^{-12}	b	5	7	8		5	7
						9	*6*	*9*	*9*	*3*	*8*
4	$C_2F_6(^*) \rightarrow 2CF_3$	$2.367T^{1.5} - 4.093\times10^2(T/500)^{3.3196}$	1.30×10^4	1.21×10^4	b						
						1		*1*	*1*		
5	$C_2F_6(^*) + M \rightarrow C_2F_6 + M$	$9.6\times10^{-12}T^{0.5}$	1.70×10^{-10}	1.66×10^{-10}	b						
						1		*1*	*1*		
6	$e^- + C_2F_6 \rightarrow CF_3 + CF_3 + e^-$	Parameter	5.00×10^{-9}	0.0	a	5	6	7		3	5
						8	*5*	*8*	*7*	*2*	*5*
7	$F + F + M \rightarrow F_2 + M$	$7.3\times10^{-32}T^{-1.0334}$	1.92×10^{-34}	2.02×10^{-34}	c		1	2			
							10	*6*			
8	$e^- + F_2 \rightarrow F + F + e^-$	$1.0\times10^{-9}T_e^{1.5}(2 + 2.7/T_e)e^{-2.7/T_e}$	1.65×10^{-8}	0.0	d	7	8	8		7	9
						8	*2*	*7*	*8*	*7*	*8*
9	$e^- + F_2 \rightarrow F + F^-$	$T_e < 0.67\ k = 6.0\times10^{-9}$ $T_e > 0.67\ k = 3.27\times10^{-9}T_e^{-3/2}$	2.92×10^{-10}	6.00×10^{-9}	e	6	6	5		7	6
						9	*5*	*8*	*4*	*7*	*5*
10	$e^- + F^- \rightarrow F + 2e^-$	$1.2\times10^{-10}T_e^{1.5}(2. + 3.45/T_e)e^{-3.45/T_e}$	1.81×10^{-9}	0.0	d						
11	$CF_3^+ + F^- \rightarrow CF_3 + F$	Estimate based on other systems	4.00×10^{-7}	4.00×10^{-7}	f	1	1	1		2	2
						4		*3*		*2*	
12	$F + F^- \rightarrow F_2 + e^-$	$1.4\times10^{-10}e^{-1.9/T_i}$	9.73×10^{-32}	0.0	g						
13	$F^- + M \rightarrow F + e^- + M$	$1.1\times10^{-10}e^{-42940/(1.16\times10^4T_i)}$	0.0	0.0	h						
14	$CF_3 + F_2 \rightarrow CF_4 + F$	Estimate based on similar reactions	3.32×10^{-12}	3.32×10^{-12}	i	7	5	6		8	6
						6	*3*	*2*	*6*	*8*	*7*
15	$CF_3 + F^- \rightarrow CF_4 + e^-$	Estimate	5.00×10^{-10}	5.00×10^{-10}	j	3	3	3		3	3
						6	*1*	*5*	*3*	*4*	*2*
16	$e^- + CF_3^+ \rightarrow CF_3$	$3.95\times10^{-9}T_e^{-0.5}T_i^{-1.0}$	4.53×10^{-8}	9.60×10^{-7}	k						
	Heterogeneous reactions										
17	$CF_3 \rightarrow CF_3(S)$	$876\ S_{CF_3}T^{0.5}/r$	3.26×10^1	3.18×10^1	l	7	4	5		7	4
						7	*3*	*6*	*6*	*7*	*4*
18	$F \rightarrow F(S)$	$0.167T^{0.5}/r$	3.11	3.03	m	6	10	10		4	8
						3	*5*	*3*	*3*	*2*	*7*
19	$F + CF_3(S) \rightarrow CF_4(S)$	$4.17\times10^{-13}\eta_F T^{0.5}$	3.69×10^{-14}	3.60×10^{-14}	n	4	7	7		3	7
						5	*3*	*6*	*6*	*4*	*6*
20	$CF_3 + CF_2(S) \rightarrow C_2F_6(S)$	$2.19\times10^{-13}\eta_{CF_3}T^{0.5}$	3.87×10^{-15}	3.78×10^{-15}							
										1	
21	$F + Si \rightarrow SiF(Si)$	$193.96T_{Si}^{0.5}/r\,\xi e^{-1258.0/T_{Si}}$(Note q)	46.1	0.0	o						
						10	*8*	*10*	*9*	*8*	*10*
22	$F + SiF(Si) \rightarrow SiF_2(Si)$	Fast	1.00	1.00							
23	$F + SiF_2(Si) \rightarrow SiF_3(Si)$	Fast	1.00	1.00							
24	$F + SiF_3(Si) \rightarrow SiF_4(Si)$	Fast	1.00	1.00							

DOCKET ALARM Find authenticated court documents without watermarks at docketalarm.com.

TABLE I. continued.

No.	Reaction	Rate expression	k_{Plasma}	$k_{Afterglow}$	Ref.	Relative sensi… Flow ~ 7 $cm^3 min^{-1}$				Flow ~ 25	
						C_2F_6	F	F_2	SiF_4	C_2F_6	F
	Surface Reactions										
25	$2F(S) \rightarrow F_2(S)$	Very fast	1.00×10^{20}	1.00×10^{20}							
26	$CF_3(S) + F(S) \rightarrow CF_4(S)$		0.0	0.0							
27	$2CF_3(S) \rightarrow C_2F_6(S)$		0.0	0.0							
	Desorption										
28	$CF_4(S) \rightarrow CF_4$	Parameter	1.00×10^{10}	1.00×10^{10}							
29	$C_2F_6(S) \rightarrow C_2F_6$	Parameter	1.00×10^{10}	1.00×10^{10}							
30	$F_2(S) \rightarrow F_2$	Parameter	1.00×10^{10}	1.00×10^{10}							
31	$F(S) \rightarrow F$	Parameter	0.0	0.0							
32	$CF_2(S) \rightarrow CF_3$	Parameter	0.0	0.0							
33	$SiF_4(Si) \rightarrow SiF_4$	Parameter	1.00×10^{10}	1.00×10^{10}							
	Simulated diffusion										
34	$e^- \rightarrow e^-(S)$	Ambipolar diffusion	3.28×10^5	2.44×10^3	p	10	10	10		10	10
						10	*6*	*9*	*7*	*10*	*9*
35	$CF_3^+ \rightarrow CF_3^+(S)$	Ambipolar diffusion	3.28×10^5	2.44×10^3	p	10	10	10		10	10
						10	*6*	*9*	*7*	*10*	*9*
36	$F^- \rightarrow F^-(S)$	Ambipolar diffusion	3.28×10^5	2.44×10^3	p	3	3	3		4	4
						2	*6*	*3*	*4*	*3*	*3*
	Surface recombination										
37	$e^-(S) + CF_3^+(S) \rightarrow CF_3(S)$	Very fast	1.00×10^{20}	1.00×10^{20}							
38	$F^-(S) + CF_3^+(S) \rightarrow CF_4(S)$	Very fast	1.00×10^{20}	1.00×10^{20}							
	Polymerization										
39	$CF_3(S) \rightarrow CF_2(P) + F(S)$	Parameter	1.00×10^2	1.00×10^2		9	10	10		9	10
						10	*8*	*10*	*10*	*10*	*10*
40	$CF_2(P) + F(S) \rightarrow CF_3(S)$	Parameter	0.0	0.0							

Note: Sensitivity entries in roman type are for systems with no silicon present. Sensitivity entries in *italic* type are for systems with silicon present.

[a] S. R. Hunter and L. G. Christophorou, J. Chem. Phys. (in press).

[b1] Reformulated from M. Rossi and D. M. Golden, Int. J. Chem. Kinet. **11**, 775 (1979).

[b2] M. Rossi (private communication).

[c1] R. K. Boyd and G. Burns, J. Phys. Chem. **83**, 88 (1979).

[c2] W. D. Breshears and R. F. Bird, J. Chem. Phys. **58**, 5176 (1971).

[d] J. S. Whittier, M. L. Lundquist, A. Ching, G. E. Thornton, and R. Hofland, Jr., J. Appl. Phys. **47**, 3542 (1976).

[e1] D. W. Trainor, J. H. Jacob, and M. Rokni, J. Chem. Phys. **72**, 3646 (1980).

[e2] D. W. Trainor and J. H. Jacob, Appl. Phys. Lett. **35**, 920 (1979).

[e3] B. Schneider and C. Brau, Appl. Phys. Lett. **33**, 569 (1978).

[f1] W. L. Nighan and W. J. Wiegand, Phys. Rev. A **10**, 992 (1974).

[f2] H. L. Chen, R. E. Center, D. W. Trainor, and W. I. Fyfe, J. Appl. Phys. **48**, 2297 (1977).

[g1] A. Mandl, J. Chem. Phys. **64**, 903 (1976).

[h] R. Hofland, Jr. and A. Mandl, J. Chem. Phys. **54**, 4129 (1971).

[i] M. J. Rossi, J. R. Barker, and D. M. Golden, J. Chem. Phys. **71**, 3722 (1979).

[j1] W. L. Nighan and W. J. Wiegand, Phys. Rev. A **10**, 992 (1974).

[j2] V. Cermak, A. Dalgarno, E. E. Ferguson, and L. Friedman, *Ion-Molecule Reactions* (Wiley-Interscience, New York, 1970).

[k] M. A. Biondi, in *Principles of Laser Plasmas*, edited by G. Bekefi (Wiley, New York, 1976), p. 125ff.

[l] Thermal impact times a sticking coefficient.

[m] P. C. Nordine and J. D. LeGrange, AIAA J. **14**, 644 (1976).

[n] Thermal impact (for F) times fractional coverage.

[o] D. L. Flamm, V. M. Donnelly, and J. A. Mucha, J. Appl. Phys. **52**, 3633 (1981).

[p1] S. C. Brown, *Introduction to Electrical Discharges in Gases* (Wiley, New York, 1966).

[p2] K. P. Suleebka and J. D. Craggs, Vacuum **24**, 557 (1974).

[p3] M. S. Naidu and A. N. Prasad, J. Phys. D. **5**, 983 (1972).

DOCKET ALARM Find authenticated court documents without watermarks at docketalarm.com.

Equation (1) is not explicitly in the chemistry, but is simulated by source and sink terms that maintain electrons and CF_3^+ ions constant throughout the plasma zone.

It is implicitly assumed that charged species are maintained by the tail of a high-energy electron energy distribution function (Vriens Model[8–10]) while electron molecule dissociation to major neutral radical channels can be attributed to electrons distributed about a lower energy. By analogy to drift tube D_e/μ_e data, we assume the that the average energy of electrons participating in reactions other than Eq. (1) is ≈ 5 eV.

C. Chemistry model

Inasmuch as possible, the chemistry model is assembled from reactions which have been reported in the literature, together with others that are assumed to occur by comparison with reactions of homologous compounds. This model is given in Table I. Note that diffusion, mentioned below, has been reformulated in terms of "chemical" rate expressions for convenience in handling by the BELLCHEM Simulation Program.[11]

The chemical reaction rate expressions which are included in Table I are gathered from many sources, as indicated in the accompanying references. In some instances these do not pertain to the cited reaction, but to a related homolog. In other cases, the references may give only a functional form for a generic class of reaction to which we have assigned numerical values based on other information. Electron temperature is difficult to define in a plasma system and the energy distribution function is almost surely non-Maxwellian, while the electron-molecule rate expressions may come from experiments done under completely unrelated conditions. These values have been used nonetheless, since the purpose of this work was to see whether such a model, however crude, bears any resemblance to real experience.

The major dissociation channel for CF_4 is taken to be

$$e + CF_4 \rightarrow CF_3 + F + e, \quad (2)$$

which, according to Winters and Inokuti,[12] proceeds only at high electron energies (12.5 eV threshold). However, recent data show that the alternative dissociative attachment reaction

$$e + CF_4 \rightarrow CF_3 + F^- \quad (3)$$

is fast ($k_a \gtrsim 10^{-10}$ cm^3/sec) at 5–6 eV (Refs. 13 and 14). Hence Eq. (3) combined with the rapid detachment reaction

$$e + F^- \rightarrow e + e + F \quad (4)$$

is equivalent to R1, Table I, and can proceed at the lower characteristic electron energies ($\approx$5–6 eV) observed in drift tube experiments.[15] Dissociation of C_2F_6 is assumed to proceed similarly and the rate is based on data from Ref. 14. CF_2 and its unsaturated derivatives are neglected as gas phase species since small amounts of CF_2 which may be formed by dissociation of CF_3 (which *a posteriori* is itself found to be present only at very low concentrations in the model) are rapidly saturated by the F atoms and F_2 which are present.[16]

D. Diffusion model

Transport of active species from the gas phase to the reacting surface is treated as an averaged loss over the entire volume. This is derived from the standard solution to the radial diffusion problem[17] and is formulated as a "residence time" (inverse of the rate constant)

$$\tau = \frac{\Lambda^2}{D}, \quad (5)$$

where the "diffusion length" Λ for the lowest mode of diffusion is

$$\Lambda = \frac{r}{2.405}. \quad (6)$$

The diffusion constant (cm^2/sec) for charged species is estimated from the ambipolar diffusion formula

$$D_A = D_+\left(1 + \frac{T_e}{T_+}\right), \quad (7)$$

where T_e and T_+ are the electron and positive ion temperatures, respectively.[18] The diffusion constant for the dominant positive charge carrier CF_3^+ is estimated as

$$D_+ = 0.00146[T_+]^{1.75}/p, \quad (8)$$

where the ion temperature T_+ is in Kelvin, and the gas pressure p is in torr. The dominant negative charge carrier in the plasma is the electron, with a diffusion constant given by

$$D_e = \frac{\mu_e k T_e}{e}, \quad (9)$$

where μ_e is the electron mobility, k is Boltzmann's constant and e is the electronic charge. The effective diffusion constant is given by

$$D_s = D_A\left(\frac{D_e + \Lambda^2\sigma_c/\epsilon_0}{D_A + \Lambda^2\sigma_c/\epsilon_0}\right). \quad (10)$$

The term in parentheses is a conductivity correction term; σ_c, the plasma conductivity, is given by

$$\sigma_c = n_e e(\mu_+ + \mu_e)$$
$$\approx n_e e \mu_e,$$

where μ_+ is the positive ion mobility, n_e the electron density, and ϵ_0 is the permittivity of free space. Under the conditions assumed for this study the correction is small and $D_s \approx D_A$.

In the afterglow, the same formulation is used, even though the simulation shows that negative ions rather than electrons may be the predominant negative carrier under some conditions. In addition, at the lower densities and temperatures there may be charge separation and spatially extended sheaths may form so that the assumed model is no longer applicable. However, the charged species decay quickly in this region so that these inaccuracies have little effect on the behavior of observable neutral species.

E. Surface interaction model

Gas phase species are adsorbed on the inert reactor wall, and these adsorbed species can react further with impinging gaseous species or with other adsorbed species and can desorb and return to the gas phase. Rates used for these processes are given in Table I. These expressions combine a surface adsorption or reaction rate with the radial diffusion estimate, and in addition contain a scaling factor that permits surface concentrations to be expressed as equivalent

DOCKET ALARM
Find authenticated court documents without watermarks at docketalarm.com.

TABLE II. CF_4 plasma on silicon; parameters and initial conditions.

		Plasma	Afterglow
Temperature	T_g	313 K	298 K
	T_i	453 K	298 K
	T_e	5.0 eV	0.025 eV
	T_{Si}	500 K	
Plasma parameters	Flow	1–80 $cm^3 min^{-1}$(STP)	
	Tube radius	0.95 cm	
	Plasma length	5.0 cm	
	Sampling distance	15.0 cm	
	ξ, Si surface fraction	0.125	
Reaction parameters	S_{CF_3}, sticking coefficient	0.002	
	η_{CF_3}, reaction efficiency	0.001	
	η_F, reaction efficiency	0.005	
Initial conditions	$[e]_0$	1.00×10^{10} cm^{-3}	
	$[CF_3^+]_0$	1.00×10^{10} cm^{-3}	
	$[F]_0$	1.00×10^{10} cm^{-3}	
	CF_4	0.50 Torr	

volume concentrations. For reactions that are characterized in Table I as "parameter," the rate constant used is an order-of-magnitude estimate. Those marked "fast" have been set sufficiently high so that they never become the rate limiting step in their reaction chain.

The reactions used to model the silicon etching process have been constructed as a sequence of single F-atom processes ultimately resulting in the formation of SiF_4 on the surface that subsequently desorbs to the gas phase. The first F-atom reaction is chosen to be the rate limiting step, in order to emulate the published rate of silicon gasification by F atoms.[1] This makes the process first order in F, maintains the proper stoichiometry, and agrees with observation. Desorption of partially fluorinated species has not been included in the model, even though gaseous SiF_2 is produced in this system.[19,20] Such species would be quickly fluorinated in the gas phase[19] so that their effect on the overall product yield is the same as that of desorbed SiF_4. Silicon, when present, was assumed to be uniformly distributed along the walls of the plasma zone, covering a fraction ξ of the total surface.

A computational problem encountered in matching wall chemistry with the gas phase flow model is that the gas "plug" advances in both space and time, while the wall remains stationary. In reality, the flowing gas mixture encounters a wall that has previously been exposed to reactive gas, and the surface concentrations of adsorbed species are determined by this history. This is not serious in the plasma region, since the wall species rapidly come to a steady state with the gas. However, in preliminary trials the afterglow region displayed an anomalous behavior where radicals recombined too rapidly, and continuously removed material from the wall. An experimental parallel exists in that a reactor must be "conditioned" for a certain time before reproducible data are obtained; this is symptomatic of the buildup of adsorbed species concentrations which thereafter remain essentially constant. These effects were modeled by setting the concentration for the major wall species, $CF_3(S)$, to that given by the steady-state relationship between reactions R17, R19, and R20 of Table I.

$$[CF_3(S)] = \frac{k_{17}[CF_3]}{k_{19}[CF_3] + k_{20}[F]}. \quad (11)$$

The concentration of $CF_3(S)$ is then constrained to this steady-state approximation value at each step of the simulation. The mass balance error caused by this open system model is less than 0.1%.

F. Polymerization model

Under some conditions of operation, a film of highly fluorinated organic material is known to form on the surface. The model allows for this occurrence and characterizes the material as $CF_2(P)$. The amount of material removed from the system in this way can be adjusted by assigning suitable values for the forward and reverse reaction rates corresponding to this process.

III. SIMULATION

The behavior of the model was calculated for the flow, pressure, and geometry in the experimental work of Smolinsky and Flamm.[3] The initial conditions and parameters selected are given in Table II. Note that temperatures are necessarily estimated. The silicon surface temperature T_{Si} was not measured and may have been much higher than the assumed value; for instance, a similar thermally-isolated sample in a stream of fluorine atoms was sometimes heated to incandescence.[21] The gas phase temperature estimate is probably reasonable, but the *effective* electron temperature T_e is somewhat uncertain. However, parametric studies show that the computation is insensitive to T_e because the rate of the dissociation reaction, Eq. (1), is set by the assumed plasma density, and the overall effect of the composite of

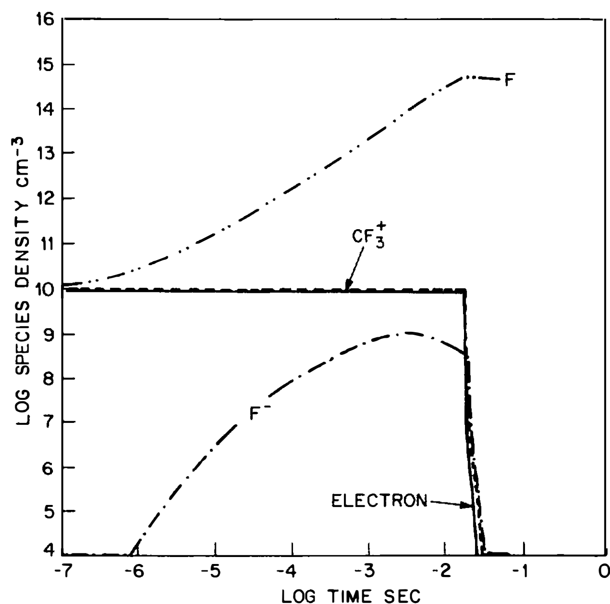

FIG. 1. Results of computer simulation of the mechanism of Table I for a CF_4 plasma with no silicon present. Pressure = 0.5 Torr, flow rate = 24.73 cc STP/min.

DOCKET ALARM
Find authenticated court documents without watermarks at docketalarm.com.

DOCKET ALARM

Explore Litigation Insights

Docket Alarm provides insights to develop a more informed litigation strategy and the peace of mind of knowing you're on top of things.

Real-Time Litigation Alerts

Keep your litigation team up-to-date with **real-time alerts** and advanced team management tools built for the enterprise, all while greatly reducing PACER spend.

Our comprehensive service means we can handle Federal, State, and Administrative courts across the country.

Advanced Docket Research

With over 230 million records, Docket Alarm's cloud-native docket research platform finds what other services can't. Coverage includes Federal, State, plus PTAB, TTAB, ITC and NLRB decisions, all in one place.

Identify arguments that have been successful in the past with full text, pinpoint searching. Link to case law cited within any court document via Fastcase.

Analytics At Your Fingertips

Learn what happened the last time a particular judge, opposing counsel or company faced cases similar to yours.

Advanced out-of-the-box PTAB and TTAB analytics are always at your fingertips.

API

Docket Alarm offers a powerful API (application programming interface) to developers that want to integrate case filings into their apps.

LAW FIRMS

Build custom dashboards for your attorneys and clients with live data direct from the court.

Automate many repetitive legal tasks like conflict checks, document management, and marketing.

FINANCIAL INSTITUTIONS

Litigation and bankruptcy checks for companies and debtors.

E-DISCOVERY AND LEGAL VENDORS

Sync your system to PACER to automate legal marketing.

WHAT WILL YOU BUILD? | sales@docketalarm.com | 1-866-77-FASTCASE

fastcase®
Smarter legal research.